

A Rate M_T Full Diversity STF Block Coded 4×4 MIMO-OFDM System with Reduced Complexity

Bhasker Gupta · Davinder S. Saini

Published online: 19 March 2013
© Springer Science+Business Media New York 2013

Abstract Multiple input multiple output (MIMO) communication systems with orthogonal frequency division multiplexing (OFDM) has a great role to play for 4G broadband wireless communications. In this paper, a space time frequency (STF) code is presented with reduced decoder complexity and to achieve code rate M_T with full diversity of $M_T M_R N_b L$ i.e., product of number of transmit antennas (M_T), receive antennas (M_R), fading blocks (N_b) and channel taps (L). The maximum achievable diversity with high rate of STF block coded MIMO-OFDM is analyzed and verified by simulation results. The decoder complexity is resolved by employing several approaches like maximum likelihood (ML), sphere decoder (SD) and array processing. The performance of STF code is compared with existing layered algebraic STF code in terms of decoder complexity and bit error rate (BER). Further, the closed form expressions for BER performance of STFBC MIMO-OFDM systems are derived and evaluated for frequency selective block fading channels with MPSK constellations.

Keywords MIMO-OFDM · STF code design · ML · SD · Array processing · BER analysis

1 Introduction

The growing demand of multimedia applications and the growth of internet related content lead to increased interest for high speed communications in practical environments like macro/micro, urban/sub-urban/rural, and indoor/outdoor. Initially, higher bandwidth was suggested for such high data rate applications. Increasing bandwidth is not a realistic method to achieve above goals and hence some spectral efficient techniques like multiple input multiple output (MIMO) systems [1,2] are designed. The key advantages of employing multiple

B. Gupta · D. S. Saini (✉)
Department of Electronics and Communication Engineering, Jaypee University of Information
Technology, Waknaghat 173234, India
e-mail: davcomm@rediffmail.com

D. S. Saini
e-mail: guptabhasker@ieee.org

antennas are (a) the improvement in reliability performance through diversity, and (b) increase in data rate through spatial multiplexing. With MIMO systems, the adverse effects of wireless propagation environment like fading can be significantly reduced. Fading mitigation can be accomplished by techniques like transmitter and receiver diversity. The signal is transmitted through multiple independent fading paths in terms of time, frequency or space and is combined constructively at the receiver.

For narrowband wireless communication systems, a number of space time (ST) codes [3–11] with various coding and modulation methods have been proposed. In ST coding, the maximum achievable diversity is equal to $M_T M_R$. In case of broadband wireless communications, the fading channel is frequency selective. Orthogonal frequency division multiplexing (OFDM) [12] is used to transform the frequency selective channel into a set of parallel frequency flat channels. In other words, high data rate stream is split into a number of low rate streams and each stream is modulated with orthogonal subcarrier. The number of subcarriers is decided such that each subcarrier should have bandwidth much less than that of coherence bandwidth of the channel. Therefore, the inter symbol interference (ISI) on each subcarrier is very small. ISI can be further mitigated by adding cyclic prefix (CP) to each OFDM symbol. Another major performance constraint in OFDM systems is inter carrier interference (ICI) [13, 14], which occurs due to carrier frequency offsets between transmitted and received carriers. Recently, the effect of ICI is estimated in OFDM systems as a function of product of f_m and T_s , frequency tracking factor (ζ) and mobile travel direction (ϵ) [15, 16]. Also ICI can be significantly reduced with the help of proper pulse shaping [17, 18]. In order to take advantage of both MIMO and OFDM modulation, MIMO-OFDM systems have been proposed. It results in two major coding approaches. The first approach is space frequency (SF) coding [19–21], where coding is applied within a single OFDM block to exploit the spatial and frequency diversities. Other one is space time frequency (STF) coding [22–25], where the coding is applied across multiple OFDM blocks to exploit the spatial, temporal, and frequency diversities available in frequency selective MIMO channels.

Earlier works on ST coding uses ST trellis codes [4] over frequency flat channels. The resulting codes achieve spatial diversity instead of full diversity. In ST coding, full diversity is equal to the product of number of transmit and receive antennas with single symbol decoding complexity [5, 6]. However, the code rate is reduced if we employ more than 2 transmit and receive antennas. It is being proved that code rate in such cases is $3/4$ [3]. To improve code rate, quasi-orthogonal STBC was proposed via a constellation rotation [7]. The code rate with such codes has upper bound of 1 but with higher decoding complexity. To reduce the complexity of code design, a grouping method [20, 26] with precoding and bit-interleaving was proposed. Recent research proposed algebraic number theory [27, 28] to construct ST codes having code rate larger than 1 but with high decoding complexity. In frequency selective channels, the full diversity is equal to $M_R M_T L$. In MIMO-OFDM, SF block coding was proposed to achieve full diversity but with code rate less than 1 [19]. The repetition mapping technique [19] used to transform existing ST codes to full diversity SF codes was also proposed but with tradeoff between diversity and symbol rate. Recently, high-rate full-diversity SF block codes have been proposed with various signal constellations and with any number of transmit antennas [29–31]. System performance can be improved further by considering coding across multiple OFDM blocks which results in STF coding [23]. STF coding exploits all of the available diversities in the spatial, temporal, and frequency domains. It is proved that a STF block coded MIMO-OFDM system can achieve a maximum diversity gain equal to the product of number of transmitting antennas, receiving antennas and multiple paths present

in the frequency selective channel. Initially, STF code design was proposed to achieve maximum diversity with rate 1 [22]. Recently, the performance of STF codes is studied under various channel conditions and system configurations [25] over quasi-static channels [22]. However, performance can be improved in terms of diversity gain if we consider general block fading channels [32,33]. In block fading channels, fading coefficients are constant over one fading block but are independent from one fading block to another. In [34], a new algebraic number theory based STF code design is proposed to achieve rate M_T in block fading channels.

The design is motivated by the fact that there is not much M_T rate ST or SF or STF codes existing that are easy to design and decode for quasi-static as well as block fading channels. In this paper, a rate M_T full diversity STF code is presented with different approach than algebraic STF codes for block fading channels. The paper addresses the issue of designing high rate SF and STF codes that are easy to design and decode. The proposed code for 4×4 MIMO system along with array processing decoder achieves goals of lower complexity as shown in Table 6. The codes behave equally well in quasi-static as well as block fading channels. Several decoding approaches like maximum likelihood (ML), sphere decoder (SD) and array processing are investigated to resolve the complexity issue. It is also proved that presented STF code achieves rate M_T and full-diversity of $M_T M_R N_b L$. The results are verified by simulation plots. Further, closed form expressions for bit error rate (BER) performance of STFBC MIMO-OFDM systems are derived and evaluated for frequency selective block fading channels with MPSK constellations.

The rest of the paper is organized as follows. In Sect. 2, a general MIMO-OFDM transceiver model is proposed. The STF performance design criteria are given in Sect. 3. In Sect. 4 the code structure and examples of rate M_T STF code are addressed. Closed form expressions for BER performance of STFBC MIMO-OFDM systems are derived in Sect. 5. In Sect. 6, various decoders are presented to reduce the system complexity. Simulation results are given in Sect. 7 and the paper is concluded in Sect. 8.

2 Space Time Frequency Coded MIMO-OFDM Systems

The various notations and symbols used in this paper are tabulated in Table 1.

A MIMO-OFDM system shown in Fig. 1 consists of M_T transmit and M_R receiving antennas.

Initially, the incoming bit stream is mapped into data symbols via modulation technique like BPSK, QPSK. The block of data symbols \mathbf{S} of size $N_C M_T N_b$ is split into J equal size sub blocks. These sub blocks can be expressed as

$$\mathbf{S} = [\mathbf{S}_1^T, \mathbf{S}_2^T, \dots, \mathbf{S}_J^T]^T \tag{1}$$

The total number of sub blocks is $J = N_C/K$, while K is given by

$$K = 2^{(\log_2 M_T L)} \tag{2}$$

Clearly for frequency selective channels, L is always greater than 1 and hence K is always a power of 4. These symbols are then encoded into STF codeword matrix $\mathbf{C} \in \mathbb{C}^{N_C \times M_T N_b}$, where codeword \mathbf{C} [22,34] can be written as

$$\mathbf{C} = [\mathbf{C}^1, \mathbf{C}^2, \dots, \mathbf{C}^{N_b}] \tag{3}$$

Table 1 Notations and symbols [matrices (vectors) are shown by bold upper (lower) case letters]

Notation	Meaning	Notation	Meaning
S	Data symbols	$\hat{\lambda}_{r_G} \hat{\lambda}_{u, r_{G_u}}$	Non-zero eigen values of matrix G and G_u
C	STF codeword matrix of size $N_C \times M_T N_b$	$\tilde{\mathbf{X}}_i$	Precoded matrix for subblock i
C^u	STF codeword matrix of size $N_C \times M_T$ during u th fading block	B_i	STF encoded matrix for subblock i
c_{M_T}^u	M_T th column vector of codeword matrix C^u	J	Number of sub blocks
$M_T(M_R)$	Number of transmitting (receiving) antennas	$\mathbf{1}_{n \times 1}$	Column matrix of 1's
N_b	Number of fading blocks	Θ^u	Unitary matrix of size $K M_T \times K M_T$, where $K = 2^{\lceil \log_2 M_T L \rceil}$
N_C	Number of sub-channels or frequency tones	BER_{MPSK}^{avg}	Average BER with MPSK Modulation
$\mathbf{H}_{i,j}^u (\alpha_{i,j}^u)$	Channel frequency response (path gains) between transmitting (i) and receiving (j) antenna during u th block	$P(\gamma)$	Probability density function (PDF)
z	Noise vector of size $N_C N_b M_R$	ζ	Frequency tracking factor
Y_j^u	Received signal at j th receive antenna during u th fading block	ε	Mobile travel direction
$(\cdot)^T$	Transpose	γ_s	Symbol SNR
$(\cdot)^H$	Hermitian transpose	R_C	Code rate of STFBC system
$\ \cdot\ _F$	Frobenius norm	Ψ	Null space of matrix
L	Number of channel taps	M	Constellation size
τ_l	Time delay of l th path	r_s	Radius of hyper-sphere
$\hat{\gamma}, \gamma$	Average and instantaneous SNR	β	Number of bits/symbol
I_{M_R}	Identity matrix of size M_R and M_R	H[↓]	Pseudo inverse of channel matrix H
\Re	Correlation matrix of channel h	Λ	Complex lattice
\otimes	Kronecker product	U	Upper triangular matrix
\circ	Hadamard product	Z_S	Unconstrained solution of Frobenius norm of Y-CH
E	Expectation operator	$d_{K_S}^2$	Distance between codeword and centre of K_S -dimensional sphere
G, G_u	Block diagonal matrix of size $N_b N_C \times N_b M_T L$ and $N_C \times M_T L$	$\hat{\mathbf{H}}_{m \times m}$	Hadamard matrix of order $m \times m$
r_G, r_{G_u}	Rank of matrix G and G_u	f_m	Maximum Doppler spread

where, the $N_C \times M_T$ matrix **C^u** is defined as $\mathbf{C}^u = [\mathbf{c}_1^u, \mathbf{c}_2^u, \dots, \mathbf{c}_{M_T}^u]$ for $u = 1, 2, \dots, N_b$. The OFDM transmitter performs an N_C -point inverse fast Fourier transform (IFFT) to each column of matrix **C^u** during the fading block u . After IFFT modulation, CP is added (with length \geq channel delay spread) to remove ISI. The information is then passed through MIMO

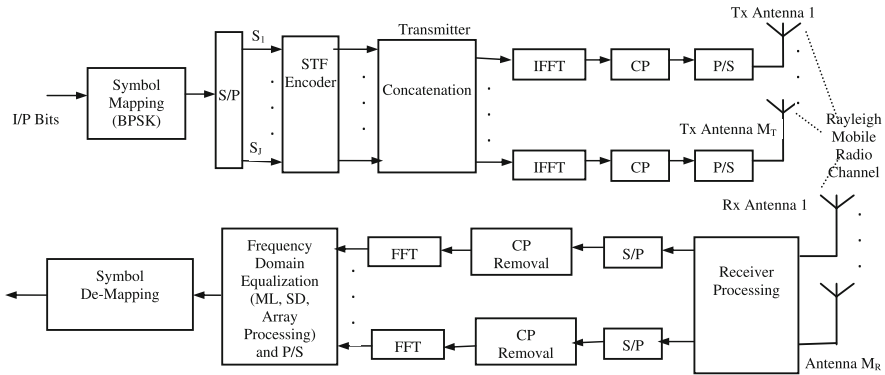


Fig. 1 MIMO-OFDM transceiver model

channel which is characterized by Jake’s model [35] as shown below for Rayleigh frequency selective channels.

$$h_{i,j}^u(t) = \sum_{l=0}^{L-1} \alpha_{i,j}^u(l) \delta(t - \tau_l) \tag{4}$$

Equation (4) represents channel impulse response (CIR) from the *i*th transmit antenna to *j*th receive antenna during *u*th fading block. The $\alpha_{i,j}^u(l)$ ’s are zero mean complex Gaussian random variables and independent for any (i, j, u, l) , where $1 \leq i \leq M_T, 1 \leq j \leq M_R, 1 \leq u \leq N_b$ and $1 \leq l \leq L - 1$. It is further assumed that all path gains follow the same power delay profile i.e. $E \left[\left[\alpha_{i,j}^u(l) \right]^2 \right] = \delta_l^2 > 0$ for any given (i, j, u, l) . The powers of *L*-paths are normalized as $\sum_{l=0}^{L-1} \delta_l^2 = 1$. The MIMO channel experiences frequency selective fading and block fading simultaneously through *L* independent paths between each pair of transmitting and receiving antenna. It is assumed that these path gains are constant over one fading block and independent from one fading block to another.

At the receiver, the received signals are assumed to be perfectly synchronized. After removing the CP and applying FFT on frequency tones, the received signal at *j*th receive antenna during *u*th fading block is given by

$$\mathbf{Y}_j^u = \sum_{i=1}^{M_T} \text{diag}(\mathbf{c}_{i,j}^u) \mathbf{H}_{i,j}^u \tag{5}$$

where \mathbf{Y}_j^u is defined as, $\mathbf{Y}_j^u = \left[y_j^u(0), y_j^u(1), \dots, y_j^u(N_c - 1) \right]^T$ power normalization and noise terms are neglected for simplification. The channel frequency response [34] is given by

$$\mathbf{H}_{i,j}^u = \mathbf{F} \mathbf{h}_{i,j}^u \tag{6}$$

where $\mathbf{H}_{i,j}^u = \left[H_{i,j}^u(0), H_{i,j}^u(1), \dots, H_{i,j}^u(N_c - 1) \right]^T$, $\mathbf{h}_{i,j}^u = \left[\alpha_{i,j}^u(0), \alpha_{i,j}^u(1), \dots, \alpha_{i,j}^u(L - 1) \right]^T$ and $\mathbf{F} = [\mathbf{f}_0, \mathbf{f}_1, \dots, \mathbf{f}_{L-1}]$. The column vector \mathbf{f}_l is defined as $\mathbf{f}_l = \left[1, \omega_l, \omega_l^2, \dots, \omega_l^{N_c-1} \right]^T$ where $\omega_l = \exp(-j2\pi \frac{\tau_l}{T_s})$ and T_s is the effective duration of

the OFDM symbol. Let $\mathbf{D}_l = \text{diag}(\mathbf{f}_l)$, which means $\mathbf{D}_l \mathbf{c}_{i,j}^u = \text{diag}(\mathbf{c}_{i,j}^u) \mathbf{f}_l$ thus (5), can be written as

$$\mathbf{Y}_j^u = \sum_{i=1}^{M_T} \left[\mathbf{D}_0 \mathbf{c}_{i,j}^u, \mathbf{D}_1 \mathbf{c}_{i,j}^u, \dots, \mathbf{D}_{L-1} \mathbf{c}_{i,j}^u \right] \mathbf{h}_{i,j}^u \tag{7}$$

By putting $\hat{\mathbf{h}}_{l,j}^u = \left[\alpha_{1,j}^u(l), \alpha_{2,j}^u(l) \dots \alpha_{M_T,j}^u(l) \right]^T$ for $l = 0, 1 \dots L-1$, (5) can be written as

$$\mathbf{Y}_j^u = \sum_{l=0}^{L-1} \left[\mathbf{D}_l \mathbf{c}_{1,j}^u, \mathbf{D}_l \mathbf{c}_{2,j}^u, \dots, \mathbf{D}_l \mathbf{c}_{M_T,j}^u \right] \hat{\mathbf{h}}_{l,j}^u \tag{8}$$

$$= \sum_{l=0}^{L-1} \mathbf{D}_l \mathbf{C}^u \hat{\mathbf{h}}_{l,j}^u \tag{9}$$

Also using

$$\mathbf{X}^u = \left[\mathbf{D}_0 \mathbf{C}^u, \mathbf{D}_1 \mathbf{C}^u, \dots, \mathbf{D}_{L-1} \mathbf{C}^u \right] \tag{10}$$

and

$$\mathbf{h}_j^u = \left[\left[\left(\hat{\mathbf{h}}_{0,j}^u \right)^T, \left(\hat{\mathbf{h}}_{1,j}^u \right)^T, \dots, \left(\hat{\mathbf{h}}_{L-1,j}^u \right)^T \right]^T \right]^T \tag{11}$$

in (7), we get $\mathbf{Y}_j^u = \mathbf{X}^u \mathbf{h}_j^u$ for $u = 1, 2, \dots, N_b$ and $j = 1, 2, \dots, M_R$. We can further generalized \mathbf{Y} , \mathbf{h} and \mathbf{X} as

$$\mathbf{Y} = \left[\left(\mathbf{Y}_1^1 \right)^T \dots \left(\mathbf{Y}_1^{N_b} \right)^T, \dots, \left(\mathbf{Y}_{M_R}^1 \right)^T \dots \left(\mathbf{Y}_{M_R}^{N_b} \right)^T \right]^T \tag{12}$$

$$\mathbf{h} = \left[\left(\mathbf{h}_1^1 \right)^T \dots \left(\mathbf{h}_1^{N_b} \right)^T \dots \left(\mathbf{h}_{M_R}^1 \right)^T \dots \left(\mathbf{h}_{M_R}^{N_b} \right)^T \right]^T \tag{13}$$

$$\mathbf{X} = \mathbf{I}_{M_R} \otimes \text{diag} \left(\mathbf{X}^1, \mathbf{X}^2 \dots \mathbf{X}^{N_b} \right) \tag{14}$$

Thus we obtain

$$\mathbf{Y} = \sqrt{\frac{\hat{\gamma}}{M_T}} \mathbf{X} \mathbf{h} + \mathbf{z} \tag{15}$$

Where the size of \mathbf{Y} , \mathbf{X} , \mathbf{h} and \mathbf{z} is $N_C N_b M_R$, $N_C N_b M_R \times M_T M_R N_b L$, $M_T M_R N_b L$ and $N_C N_b M_R$ respectively. The factor $\sqrt{\frac{\hat{\gamma}}{M_T}}$ is the power normalization factor.

3 STF Code Performance Design Criteria

Assume that \mathbf{C} and $\hat{\mathbf{C}}$ are two different STF codewords of size $N_C \times M_T N_b$ related to \mathbf{S} and $\hat{\mathbf{S}}$ respectively, the pairwise error probability (PEP) between \mathbf{C} and $\hat{\mathbf{C}}$ can be upper bounded [19] as

$$P(\mathbf{C} - \hat{\mathbf{C}}) \leq \binom{2r-1}{r} \left(\prod_{i=1}^r \lambda_i \right)^{-1} \left(\frac{\rho}{M_T} \right)^{-r} \tag{16}$$

where r is the rank of $(\mathbf{X} - \hat{\mathbf{X}})\Re(\mathbf{X} - \hat{\mathbf{X}})^H$, $\lambda_1, \dots, \lambda_r$ is the non-zero eigen values of $(\mathbf{X} - \hat{\mathbf{X}})\Re(\mathbf{X} - \hat{\mathbf{X}})^H$ and $\Re = E\{\mathbf{h}\mathbf{h}^H\}$ is the correlation matrix of \mathbf{h} . The codewords \mathbf{X} and $\hat{\mathbf{X}}$ are related to \mathbf{C} and $\hat{\mathbf{C}}$ as shown in (10). Based upon PEP criteria two general STF performance criteria are depicted as follows.

Diversity Criteria: It is also called rank criteria. It states that minimum rank of $(\mathbf{X} - \hat{\mathbf{X}})\Re(\mathbf{X} - \hat{\mathbf{X}})^H$ over all pairs of codewords \mathbf{C} and $\hat{\mathbf{C}}$ should be as large as possible.

Product Criteria: It states that minimum value of the product $\prod_{i=1}^r \lambda_i$ over all pairs of different codewords \mathbf{C} and $\hat{\mathbf{C}}$ should be maximized.

In spatially uncorrelated MIMO channels, the channel taps $\alpha_{i,j}^u(l)$ between each pair of transmit antenna i and receive antenna j are independent of each other. Thus, correlation matrix $\Re = E\{\mathbf{h}\mathbf{h}^H\}$ can be written as

$$\Re = \mathbf{I}_{M_R} \otimes \mathbf{I}_{N_b} \otimes \text{diag}(\delta_0^2, \delta_1^2, \dots, \delta_{L-1}^2) \otimes \mathbf{I}_{M_T} \tag{17}$$

Factorizing \Re as $\Re = (\Re^{1/2})(\Re^{1/2})^H$, we get $\Re^{1/2} = \mathbf{I}_{M_R} \otimes \mathbf{I}_{N_b} \otimes \text{diag}(\delta_0, \delta_1, \dots, \delta_{L-1})^{1/2} \otimes \mathbf{I}_{M_T}$. Thus from (14) and (17), we have

$$(\mathbf{X} - \hat{\mathbf{X}})\Re^{1/2} = \mathbf{I}_{M_R} \otimes \mathbf{G} \tag{18}$$

Block diagonal matrix \mathbf{G} can be further written as

$$\mathbf{G} = \text{diag}(\mathbf{G}_1, \mathbf{G}_2 \dots \mathbf{G}_{N_b}) \tag{19}$$

and the $N_C \times M_T L$ matrix \mathbf{G}_u can be represented as $\mathbf{G}_u = (\mathbf{X}_u - \hat{\mathbf{X}}_u)\text{diag}(\delta_0^2, \delta_1^2, \dots, \delta_{L-1}^2)^{1/2}$ for $u = 1, 2, \dots, N_b$. Let r_G and r_{G_u} be the rank of \mathbf{G} and \mathbf{G}_u respectively, where r_G can be represented as $r_G = \sum_{u=1}^{N_b} r_{G_u}$. Let $\hat{\lambda}_1, \hat{\lambda}_2, \dots, \hat{\lambda}_{r_G}$ and $\hat{\lambda}_{u,1}, \hat{\lambda}_{u,2}, \dots, \hat{\lambda}_{u,r_{G_u}}$ are non-zero eigen values of \mathbf{G} and \mathbf{G}_u . Thus we have $\prod_{i=1}^{r_G} \hat{\lambda}_i = \prod_{u=1}^{N_b} (\hat{\lambda}_{u,1}, \hat{\lambda}_{u,2}, \dots, \hat{\lambda}_{u,r_{G_u}})$. Further, $(\mathbf{X} - \hat{\mathbf{X}})\Re(\mathbf{X} - \hat{\mathbf{X}})^H$ can be simplified to

$$(\mathbf{X} - \hat{\mathbf{X}})\Re(\mathbf{X} - \hat{\mathbf{X}})^H = \mathbf{I}_{M_R} \otimes (\mathbf{G}\mathbf{G}^H) \tag{20}$$

The rank of $\mathbf{I}_{M_R} \otimes (\mathbf{G}\mathbf{G}^H)$ is defined as $r = r_G M_R$. Thus, the performance criteria of STF codes can be modified for frequency selective block fading as follows.

Diversity Criteria for Block Fading: It is also called sum of ranks criteria, which states that maximum transmit diversity gain is given by

$$r_G = \sum_{u=1}^{N_b} r_{G_u} \tag{21}$$

For all pairs of distinct codewords \mathbf{C} and $\hat{\mathbf{C}}$.

Product Criteria for Block Fading: Maximize the product value of

$$\prod_{i=1}^{r_G} \hat{\lambda}_i = \prod_{u=1}^{N_b} (\hat{\lambda}_{u,1}, \hat{\lambda}_{u,2}, \dots, \hat{\lambda}_{u,r_{G_u}}) \tag{22}$$

for all pairs of different codewords \mathbf{C} and $\hat{\mathbf{C}}$. The maximum value is called coding gain.

The MIMO channels will experience frequency selective fading if $L > 1$. Also, if $N_b = 1$, the design rules of STF code will turns to be of SF codes in quasi-static fading channels. Main aim is to construct high rate codes with full diversity. Full diversity is directly related

to rank of the STF codes in MIMO frequency selective block fading channels. The rank is given by

$$r = r_G M_R \leq \min (M_R N_b N_c, M_R N_b M_T L) \tag{23}$$

If we consider $N_C \geq M_T L$ then rank r can be approximated as $r \leq M_R N_b M_T L$ to achieve the full diversity. The matrix \mathbf{G} should also be full rank for every distinct pair of codewords \mathbf{C} and $\hat{\mathbf{C}}$.

4 Rate M_T STF Code Design

The coding algorithm provides different steps to design rate M_T SF and STF codes in quasi-static and block fading channels. Although some work exists in [29], but the design was not generalized for STF codes. In the proposed design the algorithm work for STF codes with SF codes as special case. Initially, the algorithm processes block wise data and precodes it by multiplying with unitary matrix, and subsequently with Hadamard matrix of order 2×2 or 4×4 . The order of Hadamard matrix depends upon number of transmitting antennas used. The processed block symbols are then concatenated to form complete codeword, which are then transmitted by M_T antennas. The design can be generalized for any number of transmitting antennas.

4.1 Code structure

The rate M_T STF code scheme is shown in Fig. 2. Initially, the block of data symbols \mathbf{S} of size $N_C M_T N_b$ is split into J equal size sub blocks. The total number of sub blocks is $J = N_C / K$, where $K = 2^{\lceil \log_2 M_T L \rceil}$.

Afterwards, each sub block data symbols \mathbf{S}_i is sent through STF encoder. The generalized STF encoder is same for every input sub block \mathbf{S}_i . The Input block \mathbf{S}_i is linearly precoded [36] with a unitary matrix Θ . The algebraic construction of unitary matrix Θ [37] per block is given by

$$\Theta^u = \frac{1}{\sqrt{KM_T N_b}} \begin{bmatrix} 1 & \theta_{1(u)}^{(u)} & \theta_{1(u)}^{2(u)} & \dots & \theta_{1(u)}^{KM_T-1(u)} \\ 1 & \theta_{2(u)}^{(u)} & \theta_{2(u)}^{2(u)} & \dots & \theta_{2(u)}^{KM_T-1(u)} \\ \dots & \dots & \dots & \dots & \dots \\ 1 & \theta_{KM_T(u)}^{(u)} & \theta_{KM_T(u)}^{2(u)} & \dots & \theta_{KM_T(u)}^{KM_T-1(u)} \end{bmatrix} \tag{24}$$

where $\theta_k = e^{j \frac{\pi(4k-3)}{2KM_T}}$, $k = 1, 2, \dots, KM_T$ and $u = 1, 2, \dots, N_b$. The precoded matrix $\tilde{\mathbf{X}}_i$ can be expressed as

$$\tilde{\mathbf{X}}_i = \Theta \mathbf{S}_i \tag{25}$$

Fig. 2 Details of rate M_T STF encoder

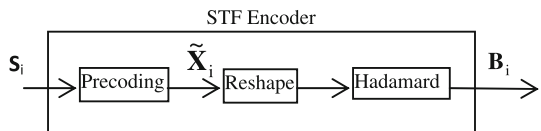


Table 2 Different values of L, K and n with $M_T = 2$ and $m = 2$

L	2	3	4	5	6	7	8
K	4	8	8	16	16	16	16
n	2	4	4	8	8	8	8

Table 3 Different values of L, K and n with $M_T = 3$ and $m = 4$

L	2	3	4	5	6	7	8
K	8	16	16	16	32	32	32
n	2	4	4	4	8	8	8

Table 4 Different values of L, K and n with $M_T = 4$ and $m = 4$

L	2	3	4	5	6	7	8
K	8	16	16	32	32	32	32
n	2	4	4	8	8	8	8

The size of $\tilde{\mathbf{X}}_i, \Theta$ and \mathbf{S}_i is $KM_T N_b$. The resultant matrix [29] is reshaped and then some matrix manipulations are performed on it as shown below

$$\mathbf{B}_i = \tilde{\mathbf{X}}_i \circ (\hat{\mathbf{H}}_{m \times M_T} \otimes \mathbf{1}_{n \times 1}) \tag{26}$$

where $\hat{\mathbf{H}}_{m \times M_T}$ is the first M_T columns of $m \times m$ Hadamard matrix $\hat{\mathbf{H}}_{m \times m}$ with $m = 2^{(\log_2 M_T)}$ and $n = K/m$. The values of m, n and K corresponding to M_T and L are given in Tables 2, 3 and 4.

Hadamard matrices of order 2 and 4 is given by

$$\hat{\mathbf{H}}_{2 \times 2} = \begin{bmatrix} 1 & 1 \\ 1 & -1 \end{bmatrix} \text{ and } \hat{\mathbf{H}}_{4 \times 4} = \begin{bmatrix} 1 & 1 & 1 & 1 \\ 1 & -1 & 1 & -1 \\ 1 & 1 & -1 & -1 \\ 1 & -1 & -1 & 1 \end{bmatrix} \tag{27}$$

Finally, \mathbf{B}_i matrices are concatenated to form codeword matrix \mathbf{C} of size $N_C \times M_T N_b$.

$$\mathbf{C} = [\mathbf{B}_1^T, \mathbf{B}_2^T \dots \mathbf{B}_J^T]^T \tag{28}$$

4.2 Simulated examples of STF Code Design

The coding strategy is same for every sub block \mathbf{B}_i^T but with some different variables so we are considering the formulation of only one sub block.

(1) When $M_T = 2$ with $N_b = 1$ and $N_b = 2$

Consider $N_C = 64$ and $L=2$. When $N_b = 1$, STF codes resembles SF codes. When $M_T = 2$, we get $K = 4, m = 2$ and $n = 2$ from Table 2. STF code corresponding to above parameters is 4×2 matrix as shown below

$$\begin{bmatrix} x_1 & x_5 \\ x_2 & x_6 \\ x_3 & -x_7 \\ x_4 & -x_8 \end{bmatrix} \tag{29}$$

where x_i 's are elements of matrix $\tilde{\mathbf{X}}_i$. It can be easily observed that 8 symbols are transmitted in 4 time slots which results in code rate of 2, which is same as that of M_T . Above code structure can be extended to more than 1 fading block by choosing $N_b = 2$. The STF code with above parameters is given as follows

$$\begin{bmatrix} x_1 & x_5 \\ x_2 & x_6 \\ x_3 & -x_7 \\ x_4 & -x_8 \end{bmatrix} \Bigg/ \begin{bmatrix} x_9 & x_{13} \\ x_{10} & x_{14} \\ x_{11} & -x_{15} \\ x_{12} & -x_{16} \end{bmatrix} \tag{30}$$

Comparing the codes in (29) and (30), upper part of code in (30) exactly resembles as that of (29) with same code rate.

(2) When $M_T = 3$ with $N_b = 1$ and $N_b = 2$

In this case, rate 3 STF code is constructed with $N_b = 1$ and $N_b = 2$. When $M_T = 3$, we can get $K = 8, m = 4$ and $n = 2$ from Table 3. STF code corresponding to above parameters is 8×3 matrix as shown below

$$\begin{bmatrix} x_1 & x_9 & x_{17} \\ x_2 & x_{10} & x_{18} \\ x_3 & -x_{11} & x_{19} \\ x_4 & -x_{12} & x_{20} \\ x_5 & x_{13} & -x_{21} \\ x_6 & x_{14} & -x_{22} \\ x_7 & -x_{15} & -x_{23} \\ x_8 & -x_{16} & -x_{24} \end{bmatrix} \tag{31}$$

Above code structure shows code rate of 3. This can be extended to more number of fading blocks, e.g., $N_b = 2$. The code structure corresponding to $N_b = 2$ is as follows

$$\begin{bmatrix} x_1 & x_9 & x_{17} \\ x_2 & x_{10} & x_{18} \\ x_3 & -x_{11} & x_{19} \\ x_4 & -x_{12} & x_{20} \\ x_5 & x_{13} & -x_{21} \\ x_6 & x_{14} & x_{22} \\ x_7 & -x_{15} & -x_{23} \\ x_8 & -x_{16} & -x_{24} \end{bmatrix} \Bigg/ \begin{bmatrix} x_{25} & x_{33} & x_{41} \\ x_{26} & x_{34} & x_{42} \\ x_{27} & -x_{35} & x_{43} \\ x_{28} & -x_{36} & x_{44} \\ x_{29} & x_{37} & -x_{45} \\ x_{30} & x_{38} & -x_{46} \\ x_{31} & -x_{39} & -x_{47} \\ x_{32} & -x_{40} & -x_{48} \end{bmatrix} \tag{32}$$

Where numerator matrix is for fading block 1 and denominator matrix is for fading block 2 with same code rate.

(3) When $M_T = 4$ with $N_b = 1$ and $N_b = 2$

The parameter corresponds to $M_T = 4$ are $K = 8, m = 4, n = 2$ as seen from Table 4. The STF code structure corresponds to above parameters is 8×4 matrix as shown below

$$\begin{bmatrix} x_1 & x_9 & x_{17} & x_{25} \\ x_2 & x_{10} & x_{18} & x_{26} \\ x_3 & -x_{11} & x_{19} & -x_{27} \\ x_4 & -x_{12} & x_{20} & -x_{28} \\ x_5 & x_{13} & -x_{21} & -x_{29} \\ x_6 & x_{14} & -x_{22} & -x_{30} \\ x_7 & -x_{15} & -x_{23} & x_{31} \\ x_8 & -x_{16} & -x_{24} & x_{32} \end{bmatrix} \tag{33}$$

The above code structure can be extended to two fading blocks as shown below with same parameters and same code rate.

$$\begin{bmatrix} X_1 & X_9 & X_{17} & X_{25} \\ X_2 & X_{10} & X_{18} & X_{26} \\ X_3 & -X_{11} & X_{19} & -X_{27} \\ X_4 & -X_{12} & X_{20} & -X_{28} \\ X_5 & X_{13} & -X_{21} & -X_{29} \\ X_6 & X_{14} & -X_{22} & -X_{30} \\ X_7 & -X_{15} & -X_{23} & X_{31} \\ X_8 & -X_{16} & -X_{24} & X_{32} \end{bmatrix} \left\| \begin{bmatrix} X_{33} & X_{41} & X_{49} & X_{57} \\ X_{34} & X_{42} & X_{50} & X_{58} \\ X_{35} & -X_{43} & X_{51} & -X_{59} \\ X_{36} & -X_{44} & X_{52} & -X_{60} \\ X_{37} & X_{45} & -X_{53} & -X_{61} \\ X_{38} & X_{46} & -X_{54} & -X_{62} \\ X_{39} & -X_{47} & -X_{55} & X_{63} \\ X_{40} & -X_{48} & -X_{56} & X_{64} \end{bmatrix} \right. \quad (34)$$

5 BER Performance of STF Coded MIMO-OFDM Systems

In this section, BER expressions for STF block coded MIMO-OFDM systems are derived and evaluated for frequency selective block fading channels. On the receiver side of MIMO-OFDM systems data can be extracted and detected through (15), The BER expression [38] can be written as

$$BER = \frac{1}{N_C} \sum_{k_0=0}^{N_C-1} BER(k_0) \quad (35)$$

Considering MPSK modulation with gray bit mapping for each subcarrier and ignoring degradation due to cyclic prefix, instantaneous BER expression for the k_0 subcarrier [39] can be represented as

$$BER_{MPSK}(k_0) = \frac{1}{\beta} \operatorname{erfc} \left(\sqrt{\gamma_s [H^2(K_0)]} \sin \left(\frac{\pi}{2\beta} \right) \right) \quad (36)$$

The exponential approximation [40] of above expression is given as

$$BER_{MPSK}(k_0) = 0.2 \exp \left(-\frac{7 \gamma_s [H(k_0)]^2}{2^{1.9\beta} + 1} \right) \quad (37)$$

Thus, BER expression in (35) can be rewritten as

$$BER_{MPSK} = \frac{1}{N_C \beta} \sum_{k_0=0}^{N_C-1} \operatorname{erfc} \left(\sqrt{\gamma_s [H^2(K_0)]} \sin \left(\frac{\pi}{2\beta} \right) \right) \quad (38)$$

and can be exponentially approximated as

$$BER_{MPSK}(k_0) = \frac{1}{N_C} \sum_{k_0=0}^{N_C-1} 0.2 \exp \left(-\frac{7 \gamma_s [H(k_0)]^2}{2^{1.9\beta} + 1} \right) \quad (39)$$

Now the average BER can be obtained by integrating BER_{MPSK} over infinite interval as shown below

$$BER_{MPSK}^{avg} = \int_0^{\infty} BER_{MPSK} P(\gamma) d\gamma \quad (40)$$

where $\gamma = [H(k_o)]^2 \gamma_s$. Since $H(k_o)$ is Rayleigh distributed with variance 1, $H(k_o)^2$ will be chi-square PDF with two degree of freedom. Consequently, put (39) in (40) we get

$$BER_{MPSK}^{avg} = 0.2 \left(1 + \frac{7 \gamma_s}{2^{1.9\beta} + 1} \right)^{-1} \tag{41}$$

In (41), BER expression for uncoded OFDM is derived. It can be extended to STF coded MIMO-OFDM systems with M_T transmitting antenna, M_R receiving antennas and N_b fading blocks. The normalized instantaneous SNR [41] in MIMO-OFDM is given as

$$\gamma = \frac{1}{M_T N_b R_C} \sum_{i=1}^{M_T} \sum_{j=1}^{M_R} \sum_{u=1}^{N_b} \sum_{l=0}^{L-1} [H_{i,j}^u(k_o, l)]^2 \gamma_s \tag{42}$$

Using above expression, BER of MPSK-STFBC-MIMO-OFDM over frequency selective block fading channels can be expressed as

$$BER_{MPSK} = \frac{1}{N_C \beta} \sum_{k_o=0}^{N_C-1} \operatorname{erfc} \left(\sqrt{\gamma_s \frac{\sum_{i=1}^{M_T} \sum_{j=1}^{M_R} \sum_{u=1}^{N_b} \sum_{l=0}^{L-1} [H_{i,j}^u(k_o, l)]^2}{R_C M_T N_b}} \sin \left(\frac{\pi}{2^\beta} \right) \right) \tag{43}$$

It can be exponentially approximated as

$$BER_{MPSK}(k_o) = \frac{0.2}{N_C} \sum_{k_o=0}^{N_C-1} \exp \left(- \frac{7 \gamma_s \sum_{i=1}^{M_T} \sum_{j=1}^{M_R} \sum_{u=1}^{N_b} \sum_{l=0}^{L-1} [H_{i,j}^u(k_o, l)]^2}{R_C M_T N_b (2^{1.9\beta} + 1)} \right) \tag{44}$$

Average BER in (40) can be extended to STFBC-MIMO-OFDM as

$$BER_{MPSK}^{avg} = \int_0^\infty \dots \int_0^\infty BER_{MPSK} \left[\begin{array}{l} P(\gamma_{1,1}^1(l)) d\gamma_{1,1}^1, \dots, P(\gamma_{M_T, M_R}^1(l)) d\gamma_{M_T, M_R}^1 \\ \dots \\ P(\gamma_{1,1}^u(l)) d\gamma_{1,1}^u, \dots, P(\gamma_{M_T, M_R}^u(l)) d\gamma_{M_T, M_R}^u \end{array} \right] \tag{45}$$

We know that $[H_{i,j}^u(k_o, l)]$ is an i.i.d (independent and identically distributed) Rayleigh channel with variance 1. Its pdf $P(\gamma_{i,j}^u(l))$ is given by

$$P(\gamma_{i,j}^u(l)) = \frac{1}{\hat{\gamma}_{i,j}^u(l)} \exp \left(- \frac{\gamma_{i,j}^u(l)}{\hat{\gamma}_{i,j}^u(l)} \right) \tag{46}$$

where $\gamma_{j,i}^u \geq 0$. Substituting (44) and (46) in (45) we get

$$BER_{MPSK}^{avg} = 0.2 \left(1 + \frac{7 \gamma_s}{R_C M_T N_b (2^{1.9\beta} + 1)} \right)^{-M_R M_T N_b L} \tag{47}$$

6 Decoding of STFBC MIMO-OFDM

Inter symbol interference caused by multipath MIMO channels distorts the MIMO-OFDM transmitted signal producing bit errors at receiver. To minimize these errors equalization or

proper decoding is needed. In this paper various equalizers or decoders like ML, SD and array processing are implemented and their performance evaluation is done in terms of BER and complexity.

6.1 Maximum Likelihood (ML)

Linear equalizers are generally used when channel does not introduce much amplitude distortion. In such situations ML [42] equalizer is chosen as it tests all possible data sequences and choose the sequence with maximum probability of occurrence. These equalizers require knowledge of channel characteristics and statistical distribution of noise in order to compute the metrics for making decisions. In ML decoding, we finds the codeword $\hat{\mathbf{C}}^u$ that solves the following minimization problem [43].

$$\hat{\mathbf{c}}^u(k_o) = \arg \min_{\mathbf{c}^u(k_o)} \sum_{u=1}^{N_b} \sum_{k_o=0}^{N_C-1} \left[\|\mathbf{Y}^u(k_o) - \mathbf{c}^u(k_o) \mathbf{H}^u(k_o)\|_F^2 \right] \tag{48}$$

The channel is assumed to be constant in one fading block. Expand (48) using Frobenius norm as follows

$$\hat{\mathbf{c}}^u(k_o) = \arg \min_{\hat{\mathbf{c}}^u(k_o)} \sum_{u=1}^{N_b} \sum_{k_o=0}^{N_C-1} \left[\text{Tr} \left| (\mathbf{Y}^u(k_o) - \mathbf{c}^u(k_o) \mathbf{H}^u(k_o))^H (\mathbf{Y}^u(k_o) - \mathbf{c}^u(k_o) \mathbf{H}^u(k_o)) \right| \right] \tag{49}$$

$$\hat{\mathbf{c}}^u(k_o) = \arg \min_{\hat{\mathbf{c}}^u(k_o)} \left[\text{Tr} \left[\begin{array}{l} (\mathbf{Y}^u(k_o))^H \mathbf{Y}^u(k_o) + (\mathbf{H}^u(k_o))^H (\mathbf{c}^u(k_o))^H \mathbf{c}^u(k_o) \mathbf{H}^u(k_o) - \\ (\mathbf{H}^u(k_o))^H (\mathbf{c}^u(k_o))^H \mathbf{Y}^u(k_o) - (\mathbf{Y}^u(k_o))^H \mathbf{c}^u(k_o) \mathbf{H}^u(k_o) \end{array} \right] \right] \tag{50}$$

If $(\mathbf{Y}^u)^H \mathbf{Y}^u$ is independent of the transmitted codeword, (50) can be written as

$$\mathbf{c}^u(k_o) = \arg \min_{\hat{\mathbf{c}}^u(k_o)} \sum_{u=1}^{N_b} \sum_{k_o=0}^{N_C-1} \left[\begin{array}{l} \text{Tr} \left[(\mathbf{H}^u(k_o))^H (\mathbf{c}^u(k_o))^H \mathbf{c}^u(k_o) \mathbf{H}^u(k_o) \right] \\ -2 \cdot \text{Real} \left(\text{Tr} \left[(\mathbf{H}^u(k_o))^H (\mathbf{c}^u(k_o))^H \mathbf{Y}^u(k_o) \right] \right) \end{array} \right] \tag{51}$$

(51) can be generalized for multiple receivers as follows

$$\hat{\mathbf{c}}^u(k_o) = \arg \min_{\hat{\mathbf{c}}^u(k_o)} \left[\begin{array}{l} \sum_{j=1}^{M_R} (\mathbf{H}_j^u(k_o))^H (\mathbf{c}^u(k_o))^H (\mathbf{c}^u(k_o)) \mathbf{H}_j^u(k_o) \\ -2 \cdot \text{Real} \left(\sum_{j=1}^{M_R} (\mathbf{H}_j^u(k_o))^H (\mathbf{c}^u(k_o))^H \mathbf{Y}_j^u(k_o) \right) \end{array} \right] \tag{52}$$

In case of ST coding, the above metric can be decomposed into two separate parts for detecting each individual symbol, i.e., ML decoding becomes single symbol decodable ML (SML). In SF coding, single symbol ML decoder doesn't yield optimum results because channel orthogonality is disturbed in case of frequency-selective channels. In such cases, joint ML decoder (JML) is preferred which detects two symbols jointly. Similarly in STF coding, we can detect two symbols jointly in one fading block which increases decoding complexity.

6.2 Sphere Decoder (SD)

As discussed above the decoding complexity is increased due to coding in three dimensions i.e. space, time and frequency. SD is preferred [44,45] in such cases. The main idea

behind SD is to limit the search space for finding the closest codeword to the particular received vector. The search space which includes optimal lattice point is given by a hyper-sphere of radius r_s centered on the received signal vector. Equation (15) can be rewritten as follows

$$\mathbf{Y} = \mathbf{C}\mathbf{H} + \mathbf{z} \tag{53}$$

Using full search for finding the optimal codeword in ML requires lot of computations which further increases with increase in constellation size, typically proportional to $2^{\beta M_T}$. Thus in SD, instead of searching all possible vectors for finding optimal codeword, we will search over a hyper-sphere of radius r_s centered on the received signal vector as shown below

$$\hat{\mathbf{C}}^u = \arg \min_{\mathbf{C}^u} [|\mathbf{Y}^u - \mathbf{C}^u \mathbf{H}^u|]_F^2 \leq r_s^2 \tag{54}$$

After optimizing $\hat{\mathbf{C}}^u$, the radius of the search sphere is reduced and above procedure is repeated till no point lie inside the search sphere. It is implemented in two steps, one is pre-processing and other is search step. In first step, we consider the solution of optimization problem mentioned in (54) is $\mathbf{Z}_S^u = (\mathbf{H}^u)^\dagger \mathbf{Y}^u$. Equation (54) can be written as

$$\min_{\mathbf{C}^u \in \Lambda} (\mathbf{C}^u - \mathbf{Z}_S^u)^H (\mathbf{H}^u)^H (\mathbf{H}^u) (\mathbf{C}^u - \mathbf{Z}_S^u) \tag{55}$$

Further, Cholskey decomposition is performed on $(\mathbf{H}^u)^H (\mathbf{H}^u)$ matrix to get upper triangular matrix as $\mathbf{U} = \{u_{k_s,1} | u_{k_s, k_s} \in r_s > 0\}$ such that $(\mathbf{H}^u)^H (\mathbf{H}^u) = (\mathbf{U}^u)^H (\mathbf{U}^u)$. The modified optimization problem is

$$[|\mathbf{U}^u (\mathbf{Z}_S^u - \mathbf{C}^u)|]^2 \leq r_s^2 \tag{56}$$

Thus, after finding unconstrained solution \mathbf{Z}_S^u and forming upper triangular matrix, a matrix \mathbf{Q}^u [45] is formed as follows

$$\mathbf{Q}^u = \left| \begin{array}{l} q_{k_s, k_s}^u = \left(u_{k_s, k_s}^u\right)^2 \\ q_{k_s, 1}^u = u_{k_s, 1}^u / u_{k_s, k_s}^u \quad k_s < 1 \end{array} \right| \tag{57}$$

In search step, the points inside the sphere are examined to locate the optimal codeword. Thus (54) can be further modified in terms of matrix \mathbf{Q} as follows

$$\sum_{i=0}^{K_s} \left| q_{i, i}^u (\mathbf{C}_i^u - \mathbf{Z}_{S_i}^u) + \sum_{j=i+1}^{K_s} q_{i, j}^u (\mathbf{C}_j^u + \mathbf{Z}_{S_i}^u) \right|^2 \leq r_s^2 \tag{58}$$

To find optimal codeword we start searching with $k_s = K_s$ and find the distance between $\mathbf{C}_{k_s}^u$ and the center of the K_s -dimensional sphere as

$$d_{k_s}^2 = \sum_{l=k}^{k_s} \left| \sum_{i=1}^{k_s} q_{l, i}^u (\mathbf{C}_i^u - \mathbf{Z}_{S_i}^u) \right|^2 \tag{59}$$

We choose another variable S_{K_s} which is defined as

$$\mathbf{S}_{K_s}^u = \mathbf{z}_{S_{K_s}}^u - \sum_{i=K_s+1}^{K_s} q_{K_s, i}^u (\mathbf{C}_i^u - \mathbf{Z}_{S_i}^u) \tag{60}$$

The condition for optimal codeword being inside the search sphere can be written as

$$d_{K_s}^2 = d_{K_s+1}^2 + q_{K_s, K_s}^u |C_{K_s}^u - S_{K_s}^u|^2 \leq r_s^2 \tag{61}$$

Thus a search space for $S_{K_s}^u$ can be specified as

$$|C_{K_s}^u - S_{K_s}^u|^2 \leq \frac{r_s^2 - d_{K_s}^2 + 1}{q_{K_s, K_s}^u} \tag{62}$$

When K_s become 1, it means a valid codeword is found. If the distance between center and the searched point is less than the radius of the hyper sphere [46], this becomes new radius. The procedure is then repeated starting again and if at any moment $d_{K_s}^2$ is greater than the radius of the sphere, the procedure is terminated.

6.3 Array Processing Decoder

In ML decoding, the pairs of transmitted symbols are detected jointly which increases decoding complexity. This complexity increases further with modulation level and with higher number of antennas employed, which in turn increases transmission delay. To overcome this problem the decoder algorithm is used along with array processing [47]. In this approach signals which are transmitted via different antennas are separated by null space. Null space decomposes received symbols into several independent parts which are decoded separately and linearly. The transmitted signals can be divided into two parts; one part is transmitted by antenna group 1 which includes 1st and 2nd transmitting antenna and other part by antenna group 2 which includes 3rd and 4th transmitting antenna. After this division, MIMO channel per fading block for $4 \times M_R$ systems can be written as $\mathbf{H}^u = [\mathbf{H}_1^u \mathbf{H}_2^u]$, where \mathbf{H}_1^u and \mathbf{H}_2^u [48] are given by

$$\mathbf{H}_1^u = \mathbf{F} \begin{bmatrix} h_{1,1}^u & h_{2,1}^u \\ h_{1,2}^u & h_{2,2}^u \\ \cdot & \cdot \\ \cdot & \cdot \\ h_{1,M_R}^u & h_{2,M_R}^u \end{bmatrix} \tag{63}$$

and

$$\mathbf{H}_2^u = \mathbf{F} \begin{bmatrix} h_{3,1}^u & h_{4,1}^u \\ h_{3,2}^u & h_{4,2}^u \\ \cdot & \cdot \\ \cdot & \cdot \\ h_{3,M_R}^u & h_{4,M_R}^u \end{bmatrix} \tag{64}$$

The null space of a matrix \mathbf{A} is the subspace of vectors \mathbf{x} for which $\mathbf{A}\mathbf{x} = 0$ and it is orthogonal complement of the range of \mathbf{A}^H . There should be more than two antennas at the receiver to ensure the existence of null space.

Ψ_1^u and Ψ_2^u denotes the null space of \mathbf{H}_1^u and \mathbf{H}_2^u respectively. Thus we have

$$\Psi_1^u (\mathbf{H}_1^u)^T = (\Psi_1^u)^T \mathbf{H}_1^u = 0 \tag{65}$$

Table 5 Number of complex valued operations in SML and JML

Parameter	SML	JML
Number of additions/subtractions	$4 + 3 \times 2^b$	$4 + 3.5 \times 2^{2b}$
Number of complex multiplications	$8 + 2.5 \times 2^b$	$10 + 4 \times 2^{2b}$

Table 6 Number of complex valued operations in SML, JML and array processing decoder

Parameter	BPSK (b = 1)		QPSK (b = 2)		16-QAM (b = 4)		16-QAM
	SML	JML	SML	JML	SML	JML	Array processing decoder [48]
Number of additions/subtractions	10	18	16	60	52	900	177
Number of complex multiplications	13	26	18	74	48	1,034	160

and

$$\Psi_2^u (\mathbf{H}_2^u)^T = (\Psi_2^u)^T \mathbf{H}_2^u = 0 \tag{66}$$

Multiplying (15) with Ψ_1^u and Ψ_2^u respectively, we get

$$(\Psi_1^u)^T \mathbf{Y}^u = (\Psi_1^u)^T \mathbf{H}^u \mathbf{X}^u + (\Psi_1^u)^T \mathbf{Z}^u \tag{67}$$

and

$$(\Psi_2^u)^T \mathbf{Y}^u = (\Psi_2^u)^T \mathbf{H}^u \mathbf{X}^u + (\Psi_2^u)^T \mathbf{Z}^u \tag{68}$$

The factor $\sqrt{\frac{\hat{\gamma}}{M_T}}$ is omitted for simplification. Using definition of null matrix [49] we have

$$(\Psi_1^u)^T \mathbf{H}^u \mathbf{X}^u = \llbracket 0 \quad (\Psi_1^u)^T \mathbf{H}_2^u \rrbracket [\mathbf{X}^u] \tag{69}$$

$$(\Psi_2^u)^T \mathbf{H}^u \mathbf{X}^u = [(\Psi_2^u)^T \mathbf{H}_1^u \quad 0] [\mathbf{X}^u] \tag{70}$$

where $[\mathbf{X}^u]$ is the rate M_T STF code given by (33) and (34) for different number of fading blocks. During decoding process, the channel matrix is repeated for all sub blocks. Hence the STF code with 4 transmit antennas can be decoded in two parallel steps. To conclude, the decoding complexity can be considerably reduced as compared to traditional ML decoding. Decoding complexity is calculated in terms of number of complex valued additions, subtractions and multiplications which are performed to decode one block of information. While one complex multiplication is considered to be equivalent to 4 real multiplications and 2 real additions, the complex addition is considered as 2 real additions. Further, the multiplication of a real valued quantity by a factor 2, like the term on right hand side of Eq. (51) is implemented using one real valued addition. In case of ML decoding, we have to compare single symbol decodable ML for ST codes and jointly decodable ML for SF and STF codes. In the first case, we need to compute 2^b metrics for each of the two transmitted symbols, where b is number of bits per modulated symbol. In joint ML, we require 2^{2b} metrics to determine symbols which jointly minimizes (51). The number of necessary complex valued additions/subtractions and multiplications are summarized in Table 5.

Table 7 Simulation parameters

Parameter	Value
Total bandwidth	20 MHz
Number of transmit antenna	2 and 4
Number of receiving antenna	2 and 4
Number of data subcarriers	64
Number of pilot-subcarriers	None
IFFT size	64
Guard period type	Cyclic extension
Cyclic prefix length	16
Carrier modulation used	BPSK-Rate-4 codes 4-QAM-Rate-2 codes
Channel model	Two-ray equal power delay profile model
Delay spread	0.2 μ s
Transmission rate	4/bits/s/Hz
Maximum Doppler spread	200 Hz
Maximum Doppler shift	$2\pi f_m = 1.256 \times 10^{-3}$
Frequency tracking factor (ζ)	$\zeta \cong 1.216 \cos \epsilon$
Direction of mobile Travel (ϵ)	In the direction of base station
Window type	Rectangular pulse

We can compute exact numbers with different modulation schemes like BPSK, QPSK and 16-QAM as shown in Table 6.

From above table, it can be concluded that complexity incases with increase in constellation size and among all decoders array processing decoder exhibits least complexity compared to ML decoders. In SD complexity is measured in terms of average floating point operations (FLOPS) which include all arithmetic operations. Average FLOPS per block in case of SD used in this paper is 10(approx.) for BPSK and increased up to 200 for 16-QAM. Thus, the FLOPS are considerably less than number of real multiplications and additions in SML and JML but more than that of array processing decoder. Thus, array processing decoder is considerably less complex than SML, JML and SD. However, total system complexity also includes complexity of other functional blocks like calculating IFFT and FFT at transmitter and receiver end. The complex multiplications required for an N-point FFT is $N \log_2 N$, which equals to 384 complex multiplications for $N = 64$. Although, decoding complexity in array processing decoder is proportional to \sqrt{M} as compared to M^2 in ML decoder but for faster decoding it requires higher power. This decoding scheme can be used even with more number of transmit antennas.

7 Simulation Results

7.1 Simulation Parameters

The parameters used for simulation of Fig. 1 are listed in Table 7.

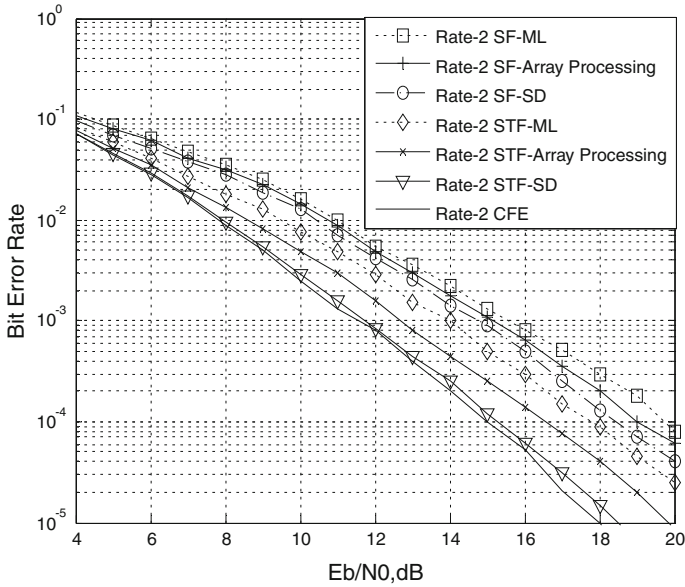


Fig. 3 BER of STFC and SFC for 2x2 MIMO-OFDM system using 4-QAM

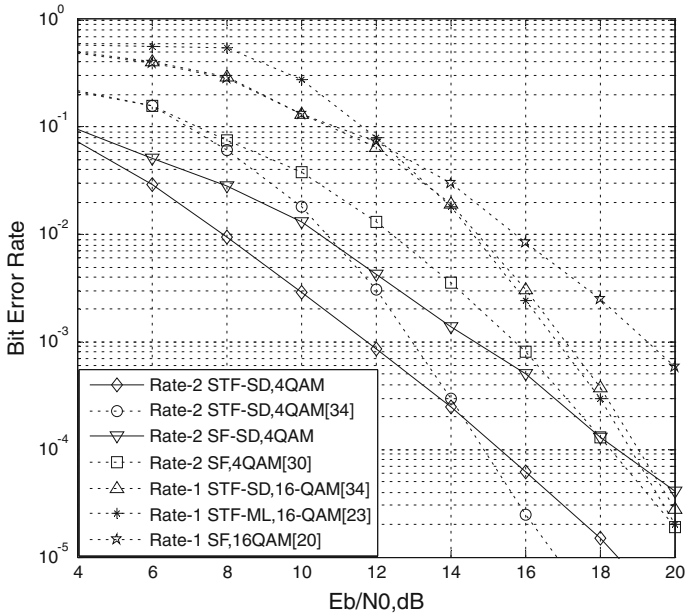


Fig. 4 BER comparison of STFC and SFC with different rates for 2x2 MIMO-OFDM

7.2 Results

In order to support analytical results and formulas derived in previous sections, we are showing simulation results by plotting BER with variation in signal to noise (SNR) ratio.

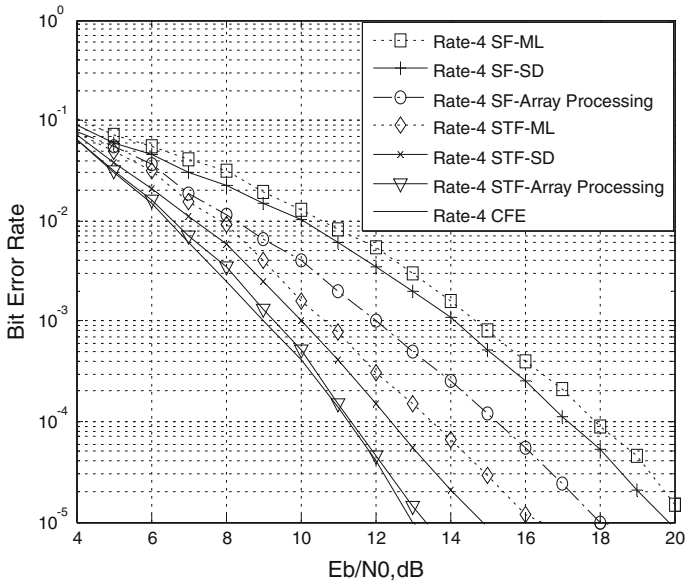


Fig. 5 BER of STFC and SFC for 4×4 MIMO-OFDM system using BPSK

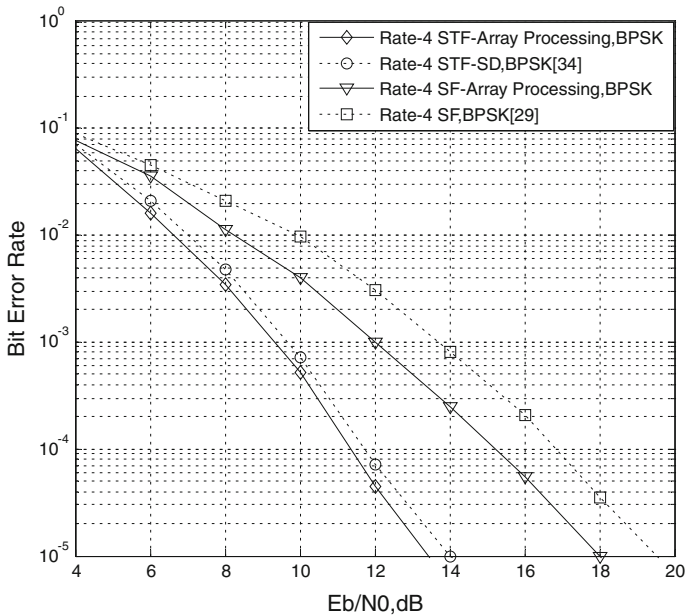


Fig. 6 BER comparison of STFC and SFC with rate-4 for 2×2 MIMO-OFDM system

Simulations are done in two phases. In phase 1, results are plotted considering two transmit and two receiving antennas, and in phase 2, with four transmit and four receiving antennas. Results are also compared with existing codes with same code rate and modulations. The simulated channel is an MIMO frequency selective block fading channel derived from simple

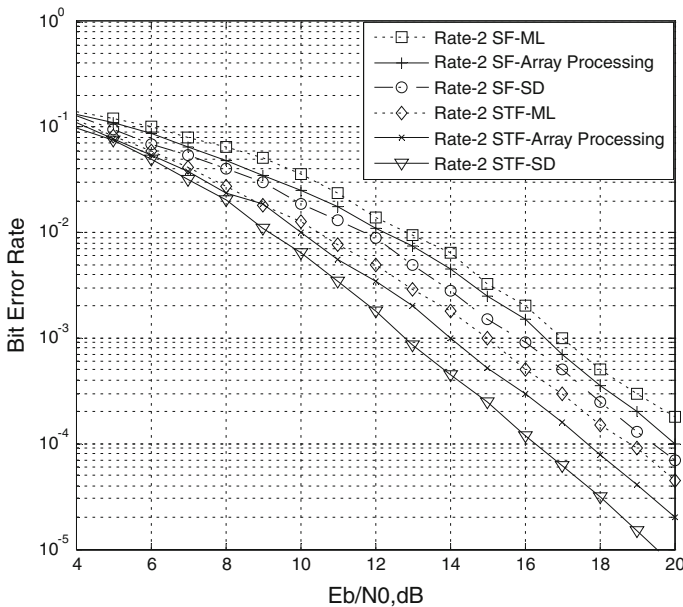


Fig. 7 BER of STFC and SFC for 2×2 MIMO-OFDM system with ICI using 4-QAM

two-ray equal power delay profile as per Jake's Model. The channel also accounts the effects of Doppler shift and Doppler spread existing due to relative motion between transmitter and receiver. Further, we assume that the receiver has perfect knowledge of the channel while transmitter doesn't know the channel.

Figure 3 shows performance comparison of rate-2 STF codes in (30) with rate-2 SF codes in (29) implemented with ML, SD and array processing decoders on receiver side. Rate-2 STF codes have larger slope curves than SF codes due to higher diversity order. Among decoders STF with SD clearly outperforms the other combinations because in array processing there is an error in calculating null-matrix with 2 receivers, and in ML, the size of search space for selecting optimum code is large. Further, it infers that the results using the closed form expression (CFE) in (47) are very close to the simulation results.

Figure 4 compares STF code in (30) with existing rate-2 STF and rate-1 STF code in [23, 34] with ML and SD on receiver side. It also compares it with rate-2 SF code in (29) and other existing rate-2 SF [30] and rate-1 SF [20] codes. To fix the transmission rate at 4/bits/sec/Hz, we employed 4-QAM modulation technique for rate-2 codes and 16-QAM for rate-1 codes. Figure 4 shows that STF code in (30) and SF code in (29) dominates in lower SNR region but STF code in [34] and SF code in [30] dominates in higher SNR region. Also Rate-2 STF curve has higher slope than SF due to higher diversity order of 16 instead of 8.

Figure 5 compares rate-4 STF codes in (34) with rate-4 SF codes in (33) both implemented in concatenation with ML, SD and array processing decoders. This implies that rate-4 STF codes with array processing decoders have better performance than all other combinations because of the benefit of calculating error-free null-matrix with 4 receiving antennas. Further, it can be seen that the results using the closed form expression in (47) are very close to the simulation results.

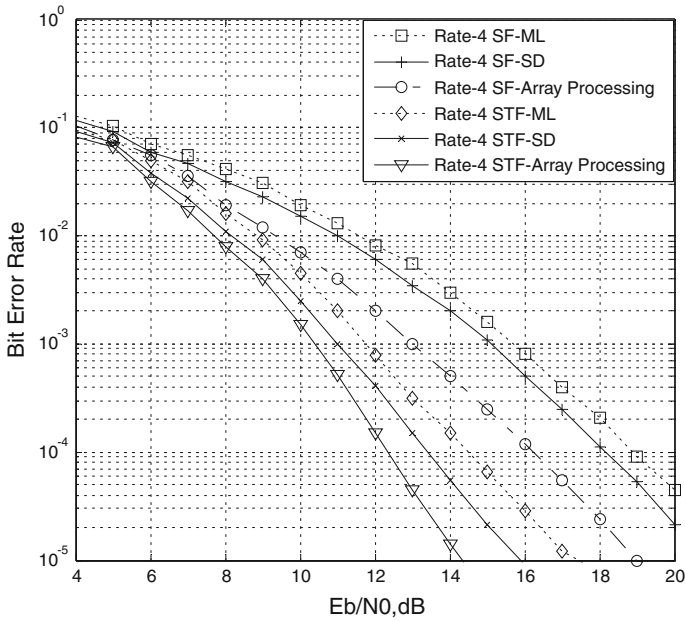


Fig. 8 BER of STFC and SFC for 4×4 MIMO-OFDM system with ICI using BPSK

Figure 6 compares STF code in (34) with existing rate-4 STF in [34] and rate-4 SF code in (33) with existing rate-4 SF code in [29]. To fix the transmission rate at 4/bits/s/Hz, we employed BPSK modulation technique for both rate-4 STF and SF codes. Figure 6 implies that STF code in (34) and SF code in (33) shows better performance than existing rate-4 STF and SF codes due to reduction in decoder complexity. BER performance can be further improved by considering higher delay spread. Figures 7 and 8 shows the effect of ICI on BER performance of rate-2 and rate-4 SF and STF codes with different decoders. Comparing Figs. 3 and 7, it is observed that the BER performance is degraded due to ICI by almost 1dB in all cases. Similar pattern is observed with rate-4 codes.

8 Conclusion

In this paper, a rate M_T full diversity STF code is presented with an approach different from algebraic STF codes in block fading channels. STF code presented in this paper is quite simple to design and easy to decode. It is also proved that STF code achieves rate M_T and full-diversity of $M_T M_R N_b L$ numerically and verified by simulation results. The performance of STF code is compared with other existing STF codes in terms of BER and decoder complexity. The decoder complexity is reduced remarkably by using array processing decoder with 4 antennas at receiver end. Also, the closed form expressions for BER performance of STFBC MIMO-OFDM systems are very close to simulation results. Work can be done to increase coding gain and to develop application based upon the presented codes.

References

1. Murch, R. D., & Letaief, K. B. (2002). Antenna systems for broadband wireless access. *IEEE Communications Magazine*, *40*, 76–83.
2. Bolcskei, H. (2006). MIMO-OFDM wireless systems: Basics, perspectives and challenges. *IEEE Wireless Communications*, *13*, 31–37.
3. Wang, H., & Xia, X. G. (2003). Upper bounds of rates of complex orthogonal space-time block codes. *IEEE Transactions on Information Technology*, *49*, 2788–2796.
4. Tarokh, V., Seshadri, N., & Calderbank, A. R. (1998). Space-time codes for high data rate wireless communication: Performance criterion and code construction. *IEEE Transactions on Information Theory*, *44*, 744–765.
5. Alamouti, S. M. (1998). A simple transmit diversity technique for wireless communications. *IEEE Journal on Selected Areas in Communications*, *16*, 1451–1458.
6. Tarokh, V., Jafarkhani, H., & Calderbank, A. R. (1999). Space-time block codes from orthogonal designs. *IEEE Transactions on Information Theory*, *45*, 1456–1467.
7. Su, W., & Xia, X. G. (2004). Signal constellations for quasi-orthogonal space-time block codes with full diversity. *IEEE Transactions on Information Theory*, *50*, 2331–2347.
8. Su, W., Xia, X. G., & Liu, K. J. R. (2004). A systematic design of high-rate complex orthogonal space-time block codes. *IEEE Communications Letters*, *8*, 380–382.
9. Fellenberg, C., & Rohling, H. (2009). Quadrature amplitude modulation for differential space-time block codes. *Springer Wireless Personal Communications*, *50*, 247–255.
10. Gupta, B., & Saini, S. D. (2012). Space-time/space-frequency/space-time-frequency block coded MIMO-OFDM system with equalizers in quasi static mobile radio channels using higher tap order. *Wireless Personal Communication*. doi:[10.1007/s11277-012-0672-9](https://doi.org/10.1007/s11277-012-0672-9).
11. Wen, H. Gong, & G., Lv, S. C., & Ho, P. H., (2011). Framework for MIMO cross-layer secure communication based on STBC. *Telecommunication Systems*. doi:[10.1007/s11235-011-9540-2](https://doi.org/10.1007/s11235-011-9540-2).
12. Li, Y., & Stuber, G. L. (2007). *Orthogonal frequency division multiplexing for wireless communications*. Berlin: Springer.
13. Le, K. N. (2011). Additional insight on SAGE-based carrier and residual frequency offset estimations in OFDM systems. *Springer Wireless Personal Communications*, *60*, 687–694.
14. Le, K. N. (2010). BER of OFDM in Rayleigh fading environments with selective diversity. *Wireless Communications and Mobile Computing*, *10*, 306–311.
15. Le, K. N. (2008). Bounds on inter-carrier interference power of OFDM in a Gaussian scattering channel. *Springer Wireless Personal Communications*, *47*, 355–362.
16. Le, K. N. (2008). Inter-carrier interference power of OFDM in a uniform scattering channel. *Computer Communications*, *31*, 3883–4230.
17. Le, K. N. (2008). Insights on ICI and its effects on performance of OFDM systems. *Digital Signal Processing*, *18*, 876–884.
18. Le, K. N., & Dabke, K. P. (2010). BER of OFDM with diversity and pulse shaping in Rayleigh fading environments. *Digital Signal Processing*, *20*, 1687–1696.
19. Su, W., Safar, Z., Olfat, M., & Liu, K. J. R. (2003). Obtaining full-diversity space-frequency codes from space-time codes via mapping. *IEEE Transactions on Signal Processing*, *51*, 2905–2916.
20. Su, W., Safar, Z., & Liu, K. J. R. (2005). Full-rate full-diversity space-frequency codes with optimum coding advantage. *IEEE Transactions on Information Theory*, *51*, 229–249.
21. Huttera, A. A., Mekrazib, S., Getuc, B. N., & Platbrooda, F. (2005). Alamouti-based space-frequency coding for OFDM. *Springer Wireless Personal Communications*, *35*, 173–185.
22. Molisch, A. F., Win, M. Z., & Winters, J. H. (2002). Space-time-frequency (STF) coding for MIMO-OFDM systems. *IEEE Communications Letters*, *6*, 370–372.
23. Liu, Z., Xin, Y., & Giannakis, G. (2002). Space-time-frequency coded OFDM over frequency selective fading channels. *IEEE Transactions on Signal Processing*, *50*, 2465–2476.
24. Su, W., Safar, Z., & Liu, K. J. R. (2005). Towards maximum achievable diversity in space, time and frequency: Performance analysis and code design. *IEEE Transactions on Wireless Communications*, *4*, 1847–1857.
25. Fozunbal, M., McLaughlin, S. W., & Schafer, R. W. (2005). On space-time-frequency coding over MIMO-OFDM systems. *IEEE Transactions on Wireless Communications*, *4*, 320–331.
26. Palou, F. R., Femenias, G., & Ramis, J. (2007). BER analysis of group-orthogonal multicarrier code-division multiplex systems. *Springer Wireless Personal Communications*, *36*, 97–105.
27. Damen, M. O., & Beaulieu, N. C. (2003). On two high-rate algebraic space time codes. *IEEE Transactions on Information Theory*, *49*, 1059–1063.

28. Sethuraman, B. A., Rajan, B. S., & Shashidhar, V. (2003). Full-diversity, high-rate space-time block codes from division algebras. *IEEE Transactions on Information Theory*, *49*, 2596–2616.
29. Zhang, W., Xia, X. G., & Ching, P. C. (2004). A design of high rate space frequency codes for MIMO-OFDM systems. In *Proceedings of the IEEE Global Telecommunication Conference*, pp. 209–213.
30. Zhang, W., Xia, X. G., Ching, P. C., & Wang, H. (2005). Rate two full diversity space frequency code design for MIMO-OFDM. In *Proceedings of the IEEE 6th workshop on signal processing advances in wireless communications*, pp. 321–325.
31. Kiran, T., & Rajan, B. S. (2005). A systematic design of high rate full diversity space frequency codes for MIMO-OFDM systems. In *Proceedings of the International Symposium on Information Theory*, pp. 2075–2079.
32. Biglieri, E., Caire, G., & Taricco, G. (2001). Limiting performance for block fading channels with multiple antennas. *IEEE Transactions on Information Theory*, *47*, 1273–1289.
33. El Gamal, H., & Hammons, A. R. Jr. (2003). On the design of algebraic space time codes for MIMO block fading channels. *IEEE Transactions on Information Theory*, *49*, 151–163.
34. Zhang, W., Xia, X. G., & Ching, P. C. (2007). High rate full diversity space time frequency codes for broadband MIMO block fading channels. *IEEE Transactions on Communications*, *55*, 25–34.
35. Jakes, W. C. (1975). *Microwave mobile communications*. London: Wiley.
36. Holakouei, R., Silva, A., & Gameiro, A. (2011). Multiuser precoding techniques for a distributed broadband wireless system. *Telecommunication Systems*. doi:10.1007/s11235-011-9496-2.
37. Giraud, X., Boutillon, E., & Belfiore, J. C. (1997). Algebraic tools to build modulation schemes for fading channels. *IEEE Transactions on Information Technology*, *43*, 938–952.
38. Xia, X. (2001). Precoded and vector OFDM robust to channel spectral nulls and with reduced cyclic prefix length in single transmit antenna system. *IEEE Transactions on Communications*, *49*, 1363–1374.
39. Proakis, J. G. (2001). *Digital communications*. New York: McGraw-Hill.
40. Chung, S. T., & Goldsmith, A. J. (2001). Degrees of freedom in adaptive modulation: A unified view. *IEEE Transactions on Communications*, *49*, 1561–1571.
41. Torabi, M., Aissa, S., & Soleymani, M. R. (2007). On the BER performance of space frequency block coded OFDM systems in fading MIMO channels. *IEEE Transactions on Wireless Communications*, *6*, 1366–1373.
42. Chang, T. H., Ma, W. K., & Chi, C. Y. (2008). Maximum-likelihood detection of orthogonal space-time block coded OFDM in unknown block fading channels. *IEEE Transactions on Signal Processing*, *56*, 1637–1649.
43. Rezk, M., & Friedlander, B. (2011). On high performance MIMO communications with imperfect channel knowledge. *IEEE Transactions on Wireless Communications*, *10*, 602–613.
44. Viterbo, E., & Boutros, J. (1999). A universal lattice code decoder for fading channel. *IEEE Transactions on Information Theory*, *45*, 1639–1642.
45. Hajjani, P., & Shafiee, H. (2005). Low complexity sphere decoding for space-frequency-coded MIMO-OFDM systems. In *Proceedings of the second IFIP international conference on wireless and optical communications, networks*, pp. 410–414.
46. Zheng, C., Chu, X., McAllister, J., & Woods, R. (2011). Real-valued fixed-complexity sphere decoder for high dimensional QAM-MIMO systems. *IEEE Transactions on Signal Processing*, *59*, 4493–4499.
47. Tarokh, V., Naguib, A., Seshadri, N., & Calderbank, A. R. (1999). Combined array processing and space time coding. *IEEE Transactions on Information Theory*, *45*, 1121–1128.
48. Jiang, C., Zhang, H., Yuan, D., & Chen, H. H. (2008). A low complexity decoding scheme for quasi-orthogonal space-time block coding. In *Proceedings of the 5th IEEE workshop on sensor array multi-channel, signal processing*, pp. 9–12.
49. Zhang, H., Yuan, D., & Chen, H. H. (2010). On array processing based quasi-orthogonal space time block coded OFDM systems. *IEEE Transactions on Vehicular Technology*, *59*, 508–513.

Author Biographies



Bhasker Gupta received B.E. degree in Electronics from Nagpur University, Nagpur, India in 2000 and M.E. degree in Electronics and Networking (with distinction) from U.I.E.T. Panjab University Campus, Chandigarh, India in 2007. He worked with PDMCE, Bahadurgarh and with BSAITM, Faridabad, Haryana, India as a Lecturer for 5 years and then with C.I.E.T., Rajpura, Jalandhar, Punjab, India for 2 years as Assistant Professor. He is currently working as a Senior Lecturer in Jaypee University, Wakhnaghat, India and pursuing his Ph.D. in “Space-Time-Frequency Processing of MIMO-OFDM Systems”.



Davinder S. Saini was born in Nalagarh, India in January 1976. He received B.E. degree in electronics and telecommunication engineering from College of Engineering Osmanabad, India in 1998. He received M.Tech. degree in communication systems from Indian Institute of Technology (IIT) Roorkee, India in 2001. He received Ph.D. degree in electronics and communication from Jaypee University of Information Technology Wakhnaghat, India in 2008. He is with Jaypee University of Information Technology Wakhnaghat since June 2002, and he is currently working as an Assistant Professor in electronics and communication department. His research areas include Channelization (OVSF) codes and optimization in WCDMA, routing algorithms and security issues in MANETs.